Date of publication xxxx 00, 0000, date of current version xxxx 00, 0000.

Digital Object Identifier 10.1109/ACCESS.2024.0429000

Improved Decarbonization Planning through Climate Resiliency Modeling

Osten Anderson[1], (Student Member, IEEE), Cameron Bracken[2], Casey D. Burleyson[2], Alex Pusch[3], and Nanpeng Yu[1], (Senior Member, IEEE)

[1]Department of Electrical and Computer Engineering, University of California, Riverside, Riverside, CA 92521 USA
[2]Pacific Northwest National Laboratory, Richland, WA 99354 USA
[3]Southern California Edison, Rosemead, CA 91770 USA

Corresponding author: Osten Anderson (e-mail: oande001@ucr.edu).

Casey Burleyson and Cameron Bracken and the load and renewable energy models were supported by the GODEEEP investment at Pacific Northwest National Laboratory (PNNL). PNNL is a multi-program national laboratory operated for the U.S. Department of Energy (DOE) by Battelle Memorial Institute under Contract No. DE-AC05-76RL01830. The views and opinions of authors expressed herein do not necessarily state or reflect those of the United States Government or any agency thereof.

ABSTRACT California has set ambitious decarbonization goals concerning both emissions and the portion of energy generated by renewable resources. However, climate change poses considerable uncertainties. Variation in load is driven both by the level of electrification as well as the impact of climate change on weather. Further, climate change stands to make weather more variable, impacting not just load but generation from renewable resources. In this paper, we approach the issue of the impacts of climate change on decarbonization planning from two perspectives. First, we look at the range of decarbonization pathways through 8 pathways that account for differences in socioeconomic development, global emissions, and warming. Second, we develop a more robust way of ensuring the reliability of energy resources planning than the commonly used planning reserve margin. We show that the proposed method can save between 6 and 14 billion dollars in investment and maintenance costs and outline critical policy implications concerning the reliance of power plants for satisfying planning reliability requirements, including the potential retirement of dozens of peaker power plants.

INDEX TERMS Climate change, decarbonization, power system planning, reliability.

Nomenclature

Sets

t, T	Index, set of hour
w, W	Index, set of representative period
w_r, W_r	Index, set of resiliency period
y, Y	Index, set of year
d, D	Index, set of probabilistic day
n, N	Index, set of net load duration
g, G	Index, set of generation and storage resources
u, U	Index, set of thermal unit
s, S	Index, set of storage resource
r, R	Index, set of renewable resource
h, H	Index, set of large hydro resource
z, Z	Index, set of balancing authority zone
l, L	Index, set of line
G_z	Subset of resources in zone z

Loads and Generation

$\mathcal{L}_{z,t}$	Load in zone z at time t (MW)
$\mathcal{NL}_{z,t}$	Net load in zone z at time t (MW)
$v_{u,t}$	On/off status of unit u at time t (1, 0)
$p_{g,t}$	Power output of resource g at time t (MW)
$\overline{P}_g$	Maximum output of resource g (MW)
$\underline{P}_g$	Minimum output of resource g (MW)
$f_{l,t}$	Flow on line l at time t (MW)
$\lambda_{l,z}$	Incidency of line l on zone z
c_l^{tx}	Wheeling cost of transmission line l ($/MWh)
$PF_{r,t}$	Production factor of renewable resource r at time t
p_r^{curt}	Curtailment of renewable resource r (MW)
c_r^{curt}	Cost of curtailment of resource r ($/MWh)
$SUC_{u,t}$	Startup cost of unit u at time t ($)
$SDC_{u,t}$	Shutdown cost of unit u at time t ($)
GCS_u	Generation cost slope of unit u ($/MWh)
GCI_u	Generation cost intercept of unit u ($/hour)

Storage

$\mathcal{M}$	Arbitrary large value
$v_{s,t}$	Storage s charge (0)/discharge (1) status at time t
$p_{s,t}^c$	Storage s rate of charge at time t (MW)
$p_{s,t}^d$	Storage s rate of discharge at time t (MW)

$C_{s,t}$	Storage s state of charge at time t (MWh)
η_s^c	Storage s charge efficiency
η_s^d	Storage s discharge efficiency
δ_s	Storage s self discharge
ϵ_s^{max}	Storage s maximum state of charge fraction

Investment

e_u^s	Slope of emissions rate of unit u (tons/MWh)
e_u^i	Intercept of emissions rate of unit u (tons/MWh)
e_l	Emissions rate associated with line l (tons/MWh)
E_y	Emissions cap in year y (tons)
$IU_{u,y}$	Install status of unit u in year y
$IU_{u,y}^p$	Planned install status of unit u in year y
$IU_{u,y}^b$	Build flag for unit u in year y
$IC_{g,y}$	Installed capacity of resource g in year y (MW)
$IC_{g,y}^p$	Planned capacity of resource g in year y (MW)
$IC_{g,y}^b$	Built capacity of resource g in year y (MW)
$IC_{g,y}^r$	Retired capacity of resource g in year y (MW)
$ICE_{s,y}$	Installed energy capacity of storage resource s in year y (MWh)
$ICE_{s,y}^p$	Planned energy capacity of storage resource s in year y (MWh)
$ICE_{s,y}^b$	Built energy capacity of storage resource s in year y (MWh)
$ICE_{s,y}^r$	Retired energy capacity of storage resource s in year y (MWh)
c_g^m	Maintenance cost of generator g ($/MW)
$c_s^{m,E}$	Energy maintenance cost of storage s ($/MWh)
$c_{g,y}^{cap}$	Capacity cost of generator g in year y ($/MW)
$c_{g,y}^{cap,E}$	Energy capacity cost of generator g in year y ($/MWh)
C_y^{gen}	Generation costs in year y ($)
C_y^m	Maintenance costs in year y($)
C_y^{inv}	Investment costs in year y ($)
ω_w	Weight of week w
ω_y	Weight of year y

Acronyms

CAISO	California Independent System Operator
ELCC	Effective load-carrying capacity
GW	Gigawatt
MILP	Mixed-integer linear program
MW	Megawatt
MWh	Megawatt-hours
NQC	Net qualifying capacity
PC	Photovoltaic
PRM	Planning reserve margin
RCP	Representative concentration Pathway
SSP	Shared socioeconomic pathway
UC	Unit commitment

I. INTRODUCTION

California has set aggressive targets for power system decarbonization through Senate Bill 100 and Senate Bill 350, establishing limits on the minimum generation from renewable resources and maximum emissions from power generation. These targets are meant to address California's contributions towards climate change mitigation. However, climate change in turn also poses adaptation challenges for these decarbonization goals.

Climate change, and the societal response to it, have a range of potential impacts on the electrical grid. The level of electrification that occurs in response to multi-sector decarbonization, such as transportation and buildings, will massively impact both the shape and magnitude of load patterns [1]. Simultaneously, climate change itself may impact the level of heating ventilation and air conditioning (HVAC) demand and the efficiency of electric assets as temperatures rise. Weather, and thus both load and renewable generation, will likely become even more volatile towards the middle of the century. This study seeks to address some of the challenges that climate change poses to the decarbonization pathways of California's electrical grid.

The impacts of climate change and associated increase in uncertainty will be examined through two lenses. The first lens is climate change pathways, with a set of scenarios that span a broad but plausible range of climate scenario uncertainty, climate model uncertainty, and socioeconomic and policy scenario uncertainty. These scenarios are derived from models in the Coupled Model Intercomparison Project Phase 6 (CMIP6) climate model archive, also utilized by the Intergovernmental Panel on Climate Change (IPCC). The second is a new approach towards ensuring resilient capacity planning, which leverages joint load-renewable generation forecasts in the face of climate change.

Large investments in electrical resources are expected over the coming decades to meet decarbonization targets. As such, capacity expansion modeling or generation expansion planning have been increasingly important for planning these investments, with models such as RESOLVE [2], Gridpath [3], and REEDS [4] used by various state agencies and load-serving entities. Due to computational limitations in capacity expansion modeling, it is typical to reduce the temporal dimension by modeling representative periods instead of all 8760 hours per year [5]. The goal of selecting representative periods is to choose a set of periods which, in tandem, best represent the year as a whole. However, some of the most stressful periods on a power grid account for only a few days per year, or may not even occur each year. Because these fringe cases account for so little of the yearly behavior, they will not naturally be selected as representative periods. However, they still must be planned for to ensure enough generation capacity is held to reliably operate the grid. Thus, it is necessary to enforce some constraint on reliability. Typically, this is done via a planning reserve margin (PRM) constraint [6]. However, this constraint is overly rigid, as the parameters of this constraint are determined exogenously to the generation portfolio optimization. Thus, this constraint could lead to generation portfolios that are either overly cautious, or fail to respond to periods of low renewable generation.

Ensuring power system planning produces generation portfolios that are reliable has been a task of increasing importance. In the past, the generation mix was dominated

by thermal units, which can generate at full-capacity except for outages or derates. This simplified reliability planning because it ensured dispatchability in resources and allowed grid operators to adjust output based on demand. As the penetration of variable renewable energy increases, reliability planning is becoming increasingly difficult due to the unpredictability of meteorological patterns and the timing of generator availability (lack of dispatchable resources). A large amount of work in recent years has been devoted towards this task as well as studying the effects of rare weather events on reliability.

PRM requirements ensure a specified amount of generation capacity is held, and are sized according to the projected peak demand. Each resource in a system contributes towards the requirement as a fraction of its nameplate capacity. In the typical formulation of this approach, this fraction conveys how much of the resource's capacity is equivalent to firm capacity, such as in [7] and California Public Utilities Commission (CPUC) resource adequacy requirements before 2018 [8]. However, for highly variable resources like wind, solar, and energy storage, distilling this complex variability into a single fraction is difficult. The behavior of wind, solar, and load are highly coupled due to the underlying weather dependency. The combined contributions of wind, solar, and energy storage are non-linear, as the contribution of storage is limited by both power and energy. To address this non-linearity, the effective load-carrying capacity (ELCC) has been proposed, and adopted by regulators including CPUC [9]. The ELCC allows for more accurate quantification of the load-carrying contributions of variable energy by accounting for the impact of renewable energy on net load. While the development of ELCC has improved PRM constraints, the parameters of this formulation are still determined exogenously, leading to inherent loss of accuracy. An overview of modern reliability studies focusing on the ELCC of renewables is given in [10]. In [6], the authors discuss the recent trend in exceeding PRM requirements, primarily due to techno-economic factors, as well as the impacts on planning studies accounting for the required and actual implemented margins. Ssengonzi et al. [11] analyze the ELCC of renewables across the United States, but neglect storage, which has a synergistic effect when coupled with variable renewables. Cole et al. [12] study resource adequacy contributions under a range of variable resource penetrations. Bera et al. [13] present a study of resource adequacy focusing on the sizing of energy storage in systems with high renewable penetration.

It is common to apply a Monte Carlo simulation approach to evaluating resource adequacy, as in [14] and the current approach used by the California Public Utilities Commission [15]. While these approaches are effective at evaluating resource adequacy of a fleet after the system planning step, it is impossible to perform system planning over such a large temporal domain without significantly sacrificing the level of modeling detail used to represent dispatch, as is done in [16].

There is also a developing body of work around the selection of extreme events within representative period selection. For example, Scott et al. [17] select extreme weather periods as initial cluster centers in representative period selection. A range of approaches to representative period selection with extreme periods is examined in [18]. In [19], extreme days are added as representative periods in a second optimization step based on the costs associated with dispatch of the portfolio in the first optimization step. The authors in [20] select extreme periods as those periods with peak load. An iterative approach to ensuring reliability is proposed in [21], with each iteration adding the day with maximum lost load as a representative period, until the portfolio satisfies reliability metrics. These works, however, do not study the inclusion of extreme periods as a direct replacement to industry-standard PRM, making the comparison of these methods difficult.

TABLE 1. Comparison of previous efforts towards reliable planning.

	Suitable for planning	Industry accepted reliability standards	Variable resource modeling
PRM	✓	✓	Poor
PRM with ELCC	✓	✓	Good
Resource Adequacy Studies	x	✓	Better
Extreme event selection	✓	x	Better
Resiliency days (proposed)	✓	✓	Better

In this study, we demonstrate that PRM-based reliability constraints are inflexible, and thus may lead to suboptimal generation fleets from planning solutions. In the case study of the California electric grid, PRM results in substantial overemphasis of thermal capacity for reliability needs. Many of the references above acknowledge the complex interactions between various classes of resources. These nuances are addressed through direct simulation of challenging dispatch conditions called resiliency periods. The comparison between the proposed work and previous efforts toward reliable planning is summarized in Table 1. The proposed method is shown to meet the level of required reliability threshold at cost savings as high as 14 billion dollars through 2045. The contributions of this study are as follows:

- Detailed study analysing how California's power system decarbonization plan is impacted by a range of socioeconomic and warming pathways.
- Development of novel resilient power system planning formulation.
- Demonstration that California's status quo planning approach may undervalue renewables and storage for reliability, leading to overreliance on gas-fired generation.

The remainder of the paper will be organized as follows. Section II will present the formulation of the planning model, including the proposed resilient planning method. Section III describes the Lagrangian relaxation-based solution methodology. Section IV discusses the numerical study and experimental results.

II. TECHNICAL METHOD

The decarbonization planning problem is formulated as a mixed-integer linear program over two timescales. The hourly timescale concerns dispatch or unit commitment, scheduling generation to meet demand and ancillary service requirements. The yearly timescale concerns investment decisions. Decarbonization is implemented through constraints on carbon emissions and renewable generation, which link the two timescales. The model described in this section is derived from [22]. The full formulation can be found in the referenced material, and a compact formulation is presented below as it pertains to the climate scenario analysis and novel climate resilient planning method. As a placeholder, Ω will be used to generically represent the constraints which are modeled but not developed in detail. Although not complete, the constraints presented here provide a general overview of the planning model, sufficient for the discussion of the scenario analysis and novel planning method. Subsection II-A formulates the unit commitment model. Then, Subsection II-B integrates unit commitment into the broader decarbonization model. Finally, Subsection II-C develops the novel method for enabling climate resilient planning.

A. UNIT COMMITMENT

Unit commitment (UC) is modeled hourly in segments of length T. In this section, UC will be discussed for an arbitrary year y and representative period w. As such, the variables in this section are formally time-indexed by the tuple (y, w, t), but the index of year and period will be hidden for brevity. In planning, constraints which link years and representative periods will be developed and will consider the full index. We will discuss in brief the constraints of unit commitment, but not formulate every constraint. The full UC formulation used can be found in [22], which is based on the formulation in [2].

1) Generation Resources

Generation resources are broken into five basic classes based on their unique operational characteristics: gas-fired thermal units, renewable resources, firm generation, large hydro, and storage resources. The full set of generation and storage resources is given as G, with these classes belonging to that set: $U, R, H, S \subset G$.

Thermal Units. Thermal units refers to combustion-based power plants. This includes coal plants, combined-cycle gas turbines, steam turbines, aeroderivative combustion turbines, and peakers. The commitment (on/off) status of thermal units is modeled as a binary $v_{u,t}$. These units are subject to many constraints, including minimum and maximum power (1), minimum uptime and downtime, startup and shutdown power limits, and ramp limits. These constraints will be considered the set Ω_u.

$$\underline{P}_u v_{u,t} \leq p_{u,t} \leq \overline{P}_u v_{u,t}, \ \forall u \in U, t \in T \tag{1}$$

Renewable and Firm Resources.

Renewable resources include utility-scale solar and wind, as well as aggregated behind-the-meter solar photovoltaic (PV). Firm resources denote biofuel, geothermal, small hydro, and nuclear. Renewable resources and firm resources are grouped together as they have broadly similar modeling characteristics, generating according to a fraction of their nameplate capacity. The generation of each resource (2) is the product of rated capacity $IC_{r,y}$ and hourly factor $PF_{r,t}$, minus curtailment $p^{curt}_{r,t}$. Firm resources are grouped with renewable resources as they have broadly similar behavior. Firm resources are not variable on the hourly scale, but some firm resources like small hydro generation vary by season. Firm resources cannot be curtailed, so $p^{curt}_{r,t} = 0$ for firm resources. There are further curtailment constraints for renewables, including for behind-the-meter solar PV. The set of all constraints of renewable and firm resources will be referred to as Ω_r.

$$p_{r,t} = IC_r \cdot PF_{r,t} - p^{curt}_{r,t}, \ \forall r \in R, t \in T \tag{2}$$

Large Hydro Units.

Dispatchable hydropower resources are referred to as large hydro units. The output of these units is given by $p_h(t)$ and is constrained by an energy budget, minimum and maximum power limits, and ramping limits. These constraints will be referred to with the set Ω_h.

Storage Resources.

Storage resources, consisting of battery and pumped storage, are an increasingly vital component of the energy resource fleet as the penetration of variable renewable resources increases. The charge/discharge status of these resources is represented by binary $v_{s,t}$, which prevents simultaneous charge and discharge and allows for enforcing duration constraints in pumped storage. This is modeled as:

$$0 \leq p^c_{s,t} \leq (1 - v_{s,t})\mathcal{M}, \ \forall s \in S, t \in T \tag{3}$$

$$0 \leq p^d_{s,t} \leq v_{s,t}\mathcal{M}, \ \forall s \in S, t \in T \tag{4}$$

The charge and discharge power of these resources are given by $p^c_{s,t}$ and $p^d_{s,t}$, respectively. The maximum output of these resources is characterized by their energy capacity (MWh) and power capacity (MW). These units are subject to minimum and maximum power and state of charge constraints, minimum duration constraints for pumped storage, and state of charge tracking (5). The full set of constraints for storage resources is given as Ω_s.

$$C_{s,t} = (1 - \delta_s)C_{s,t-1} + (p^c_{s,t}\eta^c_s - p^d_{s,t}\frac{1}{\eta^d_s}) \times 1\ hour, \quad \forall s \in S, t \in T \tag{5}$$

2) Zones and Lines

As discussed in the introduction, the present study principally concerns decarbonization within California. Accordingly, a zonal unit commitment model is used which focuses on California. The model represents the Western Interconnection in zones: the California Independent System Operator (CAISO),

three small balancing authorities in California (LADWP, IID, BANC), and two out-of-state balancing authority aggregations in the Northwest and Southwest.

Transmission is modeled using a transport model, treating line flows $f_{l,t}$ as a decision variable rather than incorporating a power flow formulation. This allows for an effective representation of zonal interconnection and greatly reduces the complexity associated with solving optimal power flow. Each line has a reference direction, and flow can be positive or negative in relation to that reference direction. The incidence of lines is given by $\lambda_{l,z}$, where 0 denotes non-incidence of line l on zone z, and +1 denotes reference direction of line l into zone z. Line flows are subject to transmission capacity limits, and the set of all transmission constraints are given by Ω_l.

3) Load and Reserve Requirements

Zonal power balance constraints enforce that, for each zone, generation and net imports are equal to load and net exports.

$$\sum_{u\in U_z} p_{u,t} + \sum_{s\in S_z}(p^d_{s,t} - p^c_{s,t}) + \sum_{r\in R_z} p_{r,t} + \sum_{h\in H_z} p_{h,t} + \sum_{l\in L} \lambda_{l,z} f_{l,t} = \mathcal{L}_{z,t}, \forall z \in Z, t \in T \quad (6)$$

To ensure reliable grid operation, CAISO must additionally provide for ancillary services. These include load following up and down, regulation up and down, spinning reserve, and frequency response. Ancillary service constraints are given as Ω_{as}.

4) Operation Cost

Finally, the total weekly cost of operation is the sum of fuel, startup and shutdown, curtailment, and transmission costs, and the objective function is given as the minimization of these costs:

$$\min \mathcal{C}^{gen} \quad (7)$$

$$\text{where } \mathcal{C}^{gen} = \sum_{t\in T}\sum_{u\in U}\Big\{SUC_{u,t} + SDC_{u,t} + (GCI_u \cdot v_{u,t} + GCS_u \cdot p_{u,t}) \times 1\,hour\Big\} \quad (8)$$

$$+[\sum_{t\in T}\sum_{l\in L} f_{l,t}\cdot c^{tx}_l + \sum_{t\in T}\sum_{r\in R} c^{curt}_r \cdot p^{curt}_{r,t}] \times 1\,hour.$$

B. DECARBONIZATION PLANNING

In this section, the unit commitment formulation developed above is integrated into decarbonization planning. Decarbonization planning incorporates dispatch over multiple periods and years, while allowing for the development and retirement of resources and constraining operation according to policy. The goal is to identify an investment strategy which minimizes the cost of investment, maintenance, and operation, while satisfying operational and policy constraints.

The present study is concentrated on decarbonization of California's electrical grid. As such, investment and policy constraints are only applied to CAISO, the main balancing authority in California. However, this formulation could readily be applied to multi-zone decarbonization efforts.

1) Investment

Candidate resources include various renewable resources, energy storage, and new higher-efficiency thermal units. Economic retirement is also considered for existing power plants. Each resource class interfaces with investment in a distinct way.

The operational status of thermal units is given by $IU_{u,y}$, and is a function of the planned status of the unit alongside build and retirement variables (9). The incremental build and retirement status of a unit is given by binary variables $IC^b_{u,y}$ and $IC^r_{u,y}$, respectively, where $IC^b_{u,y} = 1$ indicates unit u was newly built in year y. Within unit commitment, units can only turn on if operational (10).

$$IU_{u,y} = IU^p_{u,y} + \sum_{\mathcal{Y}=1}^{y}(IU^b_{u,\mathcal{Y}} - IU^r_{u,\mathcal{Y}}) \quad (9)$$

$$IU_{u,y} \geq v_{u,y,w,t},\ \forall u \in U,\ w \in W,\ t \in T \quad (10)$$

The investment of renewable and storage resources are considered continuous variables. The total installed capacity of resource r in year y is defined as (11), where $IC^b_r(y)$ is the incremental capacity added in year y. Investment in renewable capacity interfaces with dispatch through $IC_r(y)$ in (2).

$$IC_{r,y} = IC^p_{r,y} + \sum_{\mathcal{Y}=1}^{y}(IC^b_{r,\mathcal{Y}} - IC^r_{r,\mathcal{Y}}). \quad (11)$$

The installation of power (12) and energy capacity (13) for a storage resource are modeled separately through $ICE_s(y)$ and $IC_s(y)$ respectively. While most energy storage technologies do not have truly linearly-separable power and energy costs, this simplification follows the modeling in [2] and allows the model to optimize the duration of each storage resource.

$$IC_{s,y} = IC^p_{s,y} + \sum_{\mathcal{Y}=1}^{y}(IC^b_{s,\mathcal{Y}} - IC^r_{s,\mathcal{Y}}) \quad (12)$$

$$ICE_{s,y} = ICE^p_{s,y} + \sum_{\mathcal{Y}=1}^{y}(ICE^b_{s,\mathcal{Y}} - ICE^r_{s,\mathcal{Y}}) \quad (13)$$

The investment in storage interfaces with unit commitment through operational bounds. The rate of charge or discharge is limited to the installed power capacity: $p^c_{s,y,w,t} \leq IC_{s,y}$. The state of charge upper bound are limited by $C_{s,y,w,t} \leq ICE_{s,y} \cdot \epsilon^{max}_s$, and the lower bound similarly. For battery storage resources, instead of operating from 0% to 100%, some headroom and footroom is reserved in the interest of reducing degradation. The upper operational range is thus defined by ϵ^{max}_s.

2) Policy Constraints - Decarbonization

The present planning problem implements decarbonization through annual constraints on emissions and the proportion of energy supplied by renewable resources. Although the formulation is readily adaptable to multi-zonal decarbonization, we focus specifically on CAISO, and thus specify that

$z = 0$ corresponds to CAISO in order to enforce the following policy constraints only for CAISO.

In each year, the emissions associated with CAISO energy generation are limited, including energy from imports. Emissions of thermal units are modeled as proportional to fuel consumption, via a slope and intercept term e^s_u and e^i_u. Transmission emissions are proportional to the imported MWh by emission rate e_l. Transmission emissions are lower-bounded by 0 to prevent exports from reducing the total emissions.

$$E_y \geq \sum_{w\in W} \omega_w \cdot \sum_{t\in T} \Bigg(\sum_{u\in U_z} e^s_u \cdot p_{u,y,w,t} + e^i_u \cdot v_{u,y,w,t} + \sum_{l\in L} e_l \cdot \max(0, \lambda_{l,z} f_{l,y,w,t}) \Bigg), z = 0. \quad (14)$$

Renewable portfolio standards (RPS) ensure that a fraction RPS_y of the yearly total load be served by renewable resources. As certain firm resources like nuclear are grouped with renewables, a binary term $RPS^{eligible}_r$ is used to enforce eligibility towards RPS limits.

$$RPS_y \cdot \sum_{w\in W} \sum_{t\in T} \omega_w \cdot \mathcal{L}_{z,y,w,t} \leq \sum_{w\in W} \omega_w \cdot \sum_{r\in R} \sum_{t\in T} p_{r,y,w,t} \cdot RPS^{eligible}_r, z = 0 \quad (15)$$

3) Policy Constraints - Reliability

Due to the computational complexity associated with modeling 8760 hours per year, temporal downsampling is ubiquitous, and is often achieved by modeling representative periods. The goal of selecting representative periods is to choose a set of periods which, in tandem, best represent the year as a whole. However, some of the most stressful periods, and thus most important for reliability, on a power grid may be less frequent than a few days per year. Given that representative period selection is often limited to fewer than 37 days (i.e. 10% of the year), there is very low likelihood that these low-frequency, high-importance events will be selected as representative periods. However, accounting for these low-frequency periods is critical to ensure enough generation capacity is held to reliably operate the grid. Typically, this is integrated through a PRM constraint.

PRM constraints (16) ensure that the generation fleet for a given year can satisfy some factor above the forecasted peak load. Resources typically count towards the PRM requirement through a net qualifying capacity (NQC) or an ELCC. Thermal units, and firm generation, generally have an NQC close to 1, as they can typically generate at full capacity except for rare occasions when unavailable due to maintenance or other circumstances. The contributions of solar, wind, and storage, are either modeled through NQC in the simplistic case or ELCC. These resources are generally associated with rather low NQC due to the high variability of generation. In more detailed representations, contribution of variable resources is modeled as a function of decreasing value with increasing penetration. For example, California's gross load typically experiences daily summer peak around 5pm local time. With the proliferation of both behind-the-meter and utility-scale solar PV, the net load peak has shifted closer to 7pm, at which time solar generation is rapidly decreasing. Essentially, this resource is saturated at the peak load time, and installing more solar will have little to no effect on the peak net load. The ELCC of renewables and storage are given by $ELCC_y$ and $ELCC^s_y$, respectively. Further details of the calculation of ELCC can be found in [22] and [2].

$$PRM_y \leq \sum_{u\in U_z} IU_{u,y} \overline{P}_u NQC_u + ELCC^s_y + ELCC_y + \sum_{h\in H_z} IC_{h,y} NQC_h, z = 0. \quad (16)$$

4) Costs

Three main cost components are considered: investment, maintenance, and generation. These costs are assessed on a yearly basis. Investment is typically not modeled for every calendar year, so each year is associated with a weight ω_y. This weight encodes both the number of calendar years represented by y and a discount factor for the time value of money.

The cost associated with single-period dispatch was given by (8), with one $\mathcal{C}^{gen}_{y,w}$ for each $y \in Y, w \in W$. Then, the yearly cost of generation C^{gen}_y is a weighted sum of these generation costs. The weight ω_w encodes the portion of the year each $w \in W$ represents, such that $\sum_{w\in W} \omega_w \times ||T|| = 8760$. Thus, the generation cost for year y is given as:

$$\mathcal{C}^{gen}_y = \omega_y \sum_{w\in W} \omega_w C^{gen}_{y,w}. \quad (17)$$

In each year, maintenance costs $\mathcal{C}^m_y$ are assessed according to the total capacity of each resource, given by (18). Thermal units maintenance costs are assessed per unit, while renewable resource maintenance costs are assessed per MW. Storage resources have maintenance costs for both power and energy capacity, c^m_s and $c^{m,E}_s$ respectively. By allowing for economic retirement, resources that are no longer needed can be retired to avoid associated maintenance costs.

$$\mathcal{C}^m_y = \omega_y \Bigg(\sum_{u\in U} IU_{u,y} \cdot c^m_u + \sum_{s\in S} ICE_{s,y} \cdot c^{m,E}_s + \sum_{s\in S} IC_{s,y} \cdot c^m_s + \sum_{r\in R} IC_{r,y} c^m_r + \sum_{h\in H} IC_{h,y} \cdot c^m_h \Bigg) \quad (18)$$

Investment costs are annualized costs of constructing new resources, given by (19). When a resource is built, the annualized cost is charged for every subsequent year. Investment cost components are assessed based on resource capacity in the same manner as maintenance costs.

$$\mathcal{C}^{inv}_y = \Bigg(\sum_{u\in U} IU^b_{u,y} \cdot c^{cap}_{u,y} + \sum_{s\in S} IC^b_{s,y} \cdot c^{cap}_{s,y} + \sum_{s\in S} ICE^b_{s,y} \cdot c^{cap,E}_{s,y} + \sum_{r\in R} IC^b_{r,y} \cdot c^{cap}_{r,y} \Bigg) \cdot \sum_{\gamma=y}^{|Y|} \omega_\gamma \quad (19)$$

The objective function is then the sum of these cost components over all years:

$$\mathbb{O} = \sum_{y \in Y} \{\mathcal{C}_y^{gen} + \mathcal{C}_y^{m} + \mathcal{C}_y^{inv}\}. \tag{20}$$

Finally, the optimization formulation is written as the minimization of these costs, subject to all operational and investment constraints, in which $\Omega = [\Omega_u, \Omega_r, \Omega_h, \Omega_s, \Omega_l, \Omega_{as}]$:

$$\begin{aligned} &\min\ \mathbb{O} \\ &s.t., \Omega, (6)\ \forall y \in Y, w \in W, \\ &(9)-(11), (14)-(16)\ \forall y \in Y. \end{aligned} \tag{21}$$

C. PROPOSED METHOD: RESILIENCY DAYS

As discussed in Section II-B3, reliability requirements are often modeled by a yearly constraint on the fleet makeup. The goal of this constraint is to serve as a surrogate for modeling periods with extremely severe load conditions. There is an inherent loss of fidelity associated with distilling a dispatch problem into a constraint weighting capacities of resources by predetermined factors, especially considering the high variability of renewable resources. This modeling approach is very rigid and it fails to rigorously account for the correlation between load and renewable generation. As demand is expected to be served dominantly by a mix of variable renewables and storage, this is an extremely important element. This approach also fails to account for complex dispatch behaviors, such as ramping of thermal units.

Instead of constraining the fleet through predetermined factors, we propose the direct simulation of extreme load serving conditions. We adopt the name ‘‘resiliency periods" to refer to these extreme periods, as a complementary to representative periods. While representative periods seek to embody the most typical behaviors of the power system, resiliency periods seek to embody the most extreme periods in order to directly ensure that enough capacity is held to meet these demands. Similar to PRM, the rarity of resiliency period events means these do not need to be considered for operating costs or emissions constraints.

To do so, new sets are created corresponding to the resiliency period W_r and hour within each resiliency period T_r. Resiliency periods do not necessarily need to have the same length as representative periods. For example, resiliency periods could model days ($\|T_r\| = 24$), while representative periods could model weeks ($\|T\| = 168$). As with representative periods, resiliency periods link time within, but not across periods. The index of year is the same, as the resiliency requirements are enforced for each investment interval. The optimization (21) can be rewritten to incorporate these periods and omit PRM as:

$$\begin{aligned} &\min\ \mathbb{O} \\ &s.t., \Omega, (6)\ \forall t \in T, w \in W, y \in Y, \\ &\Omega, (6)\ \forall t \in T_r, w_r \in W_r, y \in Y \\ &(9)-(11), (14)-(15)\ \forall y \in Y. \end{aligned} \tag{22}$$

With this as the basic formulation behind using resiliency periods to enforce resilient planning, we can move on to discuss the selection of resiliency periods.

In general, the method described above can be used agnostic to the manner in which the resiliency periods are selected. However, it is suggested that they should reflect the accepted standards which inform PRM calculations. For example, California uses the 1-in-10 standard, stating that the expectation of loss of load should not exceed 1 event in 10 years.

Due to the increasing importance of renewable resources, we propose the use of net load as the metric by which periods are selected. Taking inspiration from the recently proposed concept of compound energy droughts [23], we propose the use of net load over various timesteps to properly capture the effects of variability in renewable energy.

Net load is a combination of data (load, renewable generation factors) and model outputs (total installed capacity of resources), so an iterative approach is required. First, the base model is solved while omitting reliability constraints (16):

$$\begin{aligned} &\min\ \mathbb{O} \\ &s.t., \Omega, (6)\ \forall t \in T, w \in W, y \in Y, \\ &(9)-(11), (14)-(15)\ \forall y \in Y. \end{aligned} \tag{23}$$

This provides baseline capacities of the various resources, which is necessary as it establishes a proper relationship between load in units of MW and unitless renewable generation factors. Net load is then defined as:

$$\mathcal{NL}_{z,y,d,t} = \mathcal{L}_{z,t} - \sum_{r \in R_z} IC_{r,y} \cdot PF_{r,y,d,t} \tag{24}$$

For each year $y \in Y$, hourly net load metrics should be calculated. For this discussion, it will be assumed that resiliency periods are selected as 24-hour days. The discussion here is immediately adaptable to periods of arbitrary length. A set of days $d \in D$ allows for a probabilistic interpretation of load and generation shapes. The size, and members, of D essentially bound the loss of load expectation. The approach developed in the following section ensures that load can be served for all days present in D. For instance, to meet or exceed the 1-in-10 standard, D should include 3650 days. This ensures that no load shedding occurs in the represented 10 years of input data. This method is readily tailored to other reliability margins.

We propose calculating the net load for each year and selecting resiliency days based on the maximum net load when averaged over a specified duration. This is operationalized by, for each day, rolling a window of length n through the day, calculating the average net load for each, and selecting the maximum (25).

$$\mathcal{NL}^n_{z,y,d} = \max\left(\frac{1}{n}\sum_{t}^{t+n} \mathcal{NL}_{z,y,d,t},\ \forall t \in [1, 24-n]\right) \tag{25}$$

Then, the day with the maximum n-hour net load is selected as a resiliency period. This highest net-load day is referred to as an n-hour net load peak.

$$W_r \leftarrow \arg\max_d \mathcal{NL}^n_{z,y,d}, \forall n \in N \tag{26}$$

By selecting droughts of various lengths, a range of behaviors in the correlation between renewable generation and load can be represented. For example, the 1-hour drought corresponds to the day with highest hourly net load and the 24-hour drought corresponds to the day with highest average net load. The set of all n-hour durations used to form the set of resiliency periods W_r is given as N.

The proposed planning method is summarized in Algorithm 1 and displayed as a flowchart in Fig. 1. First, the model is solved without PRM or other reliability constraints to establish baseline resource capacity, enabling the calculation of net load for future years. Resiliency days are then selected based on the net load peaks (26). Finally, the model is solved once again with these resiliency days integrated, given as (22).

Algorithm 1: Decarbonization with Resiliency

Solve model without PRM (23);
Calculate net loads $\mathcal{NL}^n_{z,y,d}$ (24);
Select resiliency days (26);
Solve model with resiliency days (22);

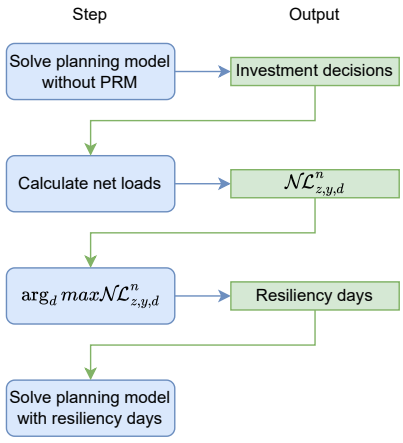

FIGURE 1. Flowchart showing the proposed method for selecting and planning with resiliency periods.

III. SOLUTION METHODOLOGY

Each of the optimization problems ((21), (22), (23)) are MILP problems. Although commercial optimization solvers have seen considerable performance improvements over recent years, MILP models still generally suffer from combinatorial complexity; computation time increases superlinearly with increase in number of variables. While small MILP models, like daily unit commitment, can be solved by commercial solvers without difficulty, planning models quickly become intractable due to their large temporal scope. To alleviate this, it is common in power system planning to simplify the model by reducing its level of detail, by some combination of reduced temporal scope, relaxation of binary variables, and clustering of thermal units. While this is effective at improving computation tractability, it reduces the fidelity between dispatch in the planning model and real-world operation. Instead, surrogate Lagrangian relaxation is employed to ensure the computational tractability of the highly detailed MILP model. Although not a contribution of this work, being derived from the solution methodology in [22], a brief overview of the technique is provided for compactness.

We will develop the method with respect to the planning model with PRM (21). The solution method can be similarly applied to the proposed resilient planning model (22). This approach begins by relaxing constraints in the primal problem (21) to form a relaxed or dual problem. In our case, we relax the zonal power balance constraints (6). Then, the violation of the relaxed constraint is incorporated into the objective function as the product of Lagrangian multipliers Λ. The vector of constraint violations is given by $\mathbf{R} = [r_{z,y,w,t}, \forall z \in Z, y \in Y, w \in W, t \in T]$. Each constraint violation is given by $r_{z,y,w,t} = \sum_{u \in U_z} p_{u,y,w,t} + \sum_{s \in S_z} (p^d_{s,y,w,t} - p^c_{s,y,w,t}) + \sum_{r \in R_z} p_{r,y,w,t} + \sum_{h \in H_z} p_{h,y,w,t} + \sum_{l \in L} \lambda_{l,z} f_{l,y,w,t} - \mathcal{L}_{z,y,w,t}$. Finally, the dual problem is given by:

$$\begin{aligned} &\min \{\mathbb{O} + \Lambda \cdot R\} \\ &s.t., \Omega \; \forall y \in Y, w \in W, \\ &(9) - (11), (14) - (16) \; \forall y \in Y. \end{aligned} \tag{27}$$

The fundamental idea of surrogate Lagrangian relaxation is to iteratively solve the dual problem (27) while updating the multipliers Λ according to the subgradients given by the constraint violations $\mathbf{R}$. In each iteration, rather than solving the full problem over all decision variables, the variables of only a small sample of thermal units are optimized, while the remainder are fixed. All variables related to other resources are optimized in each iteration. Thus, the performance increase of the method comes both from the relaxation of a complex constraint and the combinatorial unwinding of binary variables. For further discussion and details on the implementation of surrogate Lagrangian relaxation for decarbonization planning, please see [22].

The surrogate Lagrangian relaxation method is guaranteed to converge towards the optimal dual value, but it is both difficult and unnecessary to converge to zero constraint violation. Instead, when the constraint violations are sufficiently low, the thermal unit dispatch status are applied to the primal problem. By solving the primal problem with a majority of thermal units fixed to these values, a near-optimal solution to the primal problem can be obtained in relatively low CPU time.

In practice, only constraints from the representative periods and not the resiliency periods are relaxed. The total number

of resiliency hours should be much less than the total number of representative hours. Resiliency periods also interface slightly less with the objective function, as the resiliency periods' dispatch costs are not included. It should be understood that there is nothing preventing power balance constraints in the resiliency periods from being relaxed as well.

IV. NUMERICAL STUDY

In this section, we present a numerical study of the impacts of climate, socioeconomic pathways, and the proposed resilient planning method. First, the climate-generation-load dataset which enables this study is discussed. Next, we examine the planning results under a variety of scenarios. Then, a comparison of planning results under the status quo PRM reliability formulation and the proposed resiliency periods formulation is presented. Finally, we outline some of the policy implications of this study.

Outside of the climate dataset described next, the data used in this study is taken from the RESOLVE implementation published by the California Public Utilities Commissions [2]. This includes operational data, such as sizes and characteristics of existing generators, economic data, such as fuel costs and cost of new capacity, and policy data, such as emissions limits. Investment is modeled from 2025 through 2045 in 5-year intervals, with financing through 2065. We model representative periods of 3-day length and resiliency periods of 1-day length. Representative periods are selected using the approach in [5]. Resiliency periods are selected for net load peak durations of 1, 4, 12, and 24 hours. For the resiliency periods in (22), we also account for a 5% derate for generators in the resiliency period, based on the NQC for these units defined in [2].

A. CLIMATE, LOAD, AND GENERATION DATASETS

This study is enabled by recent publicly-available load and renewable generation projection datasets developed by multiple projects at the Pacific Northwest National Laboratory [24]. Load and renewable generation projections are considered in tandem, and because they are both based on the same underlying climate projections, the time series will be properly correlated. The correlation between load and renewable generation is important, so we specifically avoid Monte Carlo approaches which generally sever this correlation. As noted in [23], there are correlations between periods of high load and low renewable generation which may have extremely large impact for future grids relying heavily on variable renewables. The renewable generation projections also account for climate impacts such as solar panel efficiency loss as temperatures increase and the suppression of wind generation under high pressure conditions.

The climate, load, and generation projections are based on 40-years (1980-2019) of historical meteorology. The use of historical meteorology results in the dataset containing actual historical extreme events. The climate methodology then takes the 40-year sequence of historical weather and repeats it twice into the future (from 2020-2059 and again from 2060-2099) for eight unique scenarios that reflect a wide but plausible range of future climate and socioeconomic conditions. The details of this approach are provided in [25]. The eight future scenarios are defined jointly by a combination of Representative Concentration Pathway (RCPs 4.5 and 8.5) and Shared Socioeconomic Pathway (SSPs 3 and 5). They also reflect a range of climate model uncertainties by using warming levels from climate models that are hotter and cooler than the multimodel mean.

The RCP scenario impacts load through both climate-related impacts, such as higher temperatures increasing the load from air conditioning, as well as the level of electrification needed to meet the emissions target. The SSPs impact load through the level of consumption, economic expansion and population growth. The RCP and the warming levels both affect the production factors of renewable generation though both technological (e.g. solar panel derating) and climate (e.g. heat dome wind suppression), while maintaining physical consistency.

The RCP 4.5 and 8.5 pathways are denoted by R4 and R8, respectively. The SSP 3 and 5 pathways are denoted by S3 and S5, respectively. The cooler and hotter climate model outcomes are denoted by the suffixes "C" and "H", respectively (i.e. R4S3C, R4S3H). Details of the various scenarios are provided in [26].

To produce the data used in this study, the 40 years of historical and 80 years of future meteorology across the eight scenarios are then run through a series of load and renewable generation models to produce hourly time series of historical and projected load and renewable generation. The load projection model accounts for the hour-to-hour variations in demand due to weather (including extreme events like heat waves and cold snaps) and grows loads over time to reflect longer-term changes in population, economics, and energy policy (for example, electrification needs to stay on an RCP 4.5 pathway). For each 1/8th degree grid cell, a hypothetical wind and solar plant was modeled with generic assumptions about solar panel and wind turbine configurations. The details of the models used in this process are provided in [23] and [26]. Each scenario takes approximately 3 hours to solve in the climate pathways case, and approximate 5 hours for planning with resiliency periods, due to the increased number of simulated hours.

B. RESULTS

1) Climate Pathways

First, we examine the impacts of each of the scenarios on the 2045 fleets. The newly installed capacity in CAISO in each scenario is shown in Fig. 2. It is not surprising that different pathways force different levels of investment based on the amount of associated load growth. These results do, however, emphasize the need to account for the wide range of planning outcomes of different pathways. The buildout of renewables is as low as 50GW and as high as 87.5GW, and the buildout of energy storage is as low as 32.6GW and as high as 47GW. It is vital that this range is understood, even if these extremes

represent relatively less-likely scenarios. The investment over time is shown in Fig. 3 for both warming pathways of two of the climate scenarios. Not only do warming pathways affect the total amount of clean capacity needed to achieve decarbonization by 2045, but also the optimal intervals in which to make these investments, with both hotter scenarios favoring later investment as compared to their cooler counterparts.

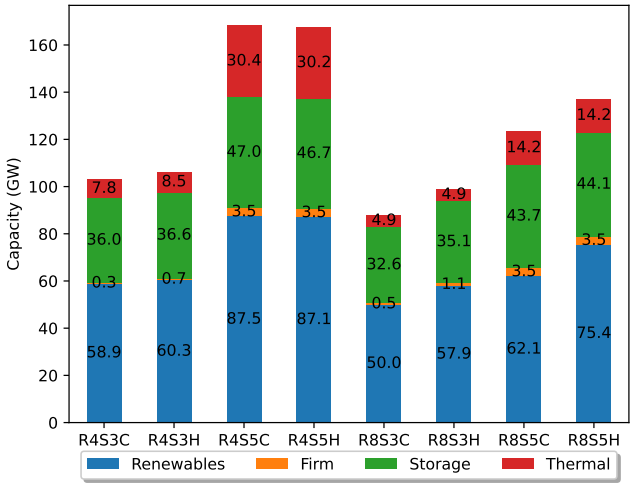

FIGURE 2. **Comparison of capacity added to CAISO fleet under different climate pathways, demonstrating the extreme variation in required capacity.**

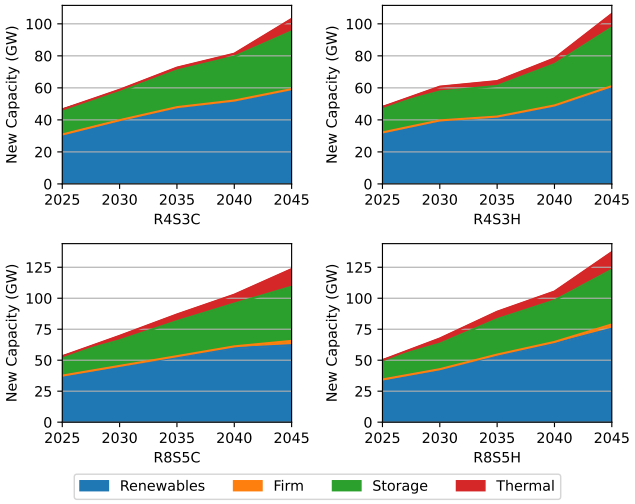

FIGURE 3. **Comparison of investment over time for the R4S3 and R8S5 scenarios with both cooler and hotter warming pathways.**

The evolution of the fleet can also be evaluated through its spatial distribution. Fig. 4 shows maps of the investment in storage and renewable projects for two years and two scenarios. These two scenarios are the most moderate of the four pathways examined. In 2030, there are relatively few differences between the two scenarios. In 2045, the differences become apparent, with substantially more investment in solar in southern California, more wind in southern Nevada, and more storage in both northern and southern California for the R8S5H scenario compared to the R4S5H scenario.

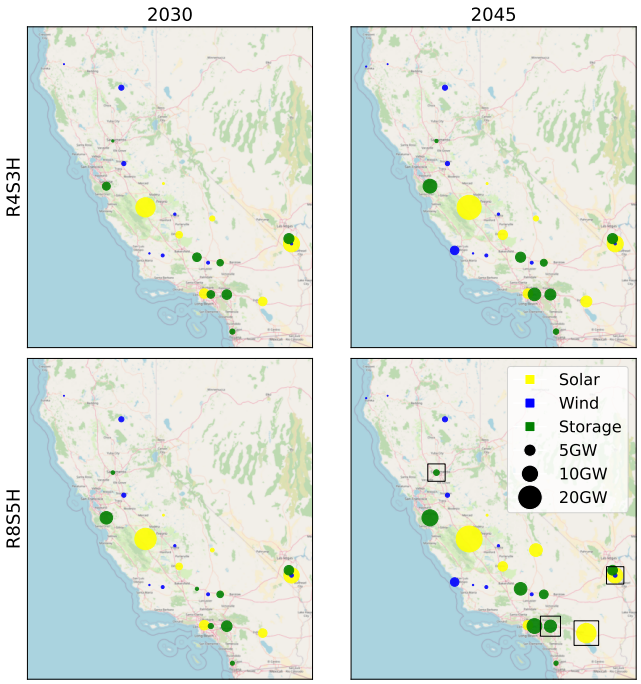

FIGURE 4. **Map depicting the installation of storage and renewable projects for 2030 and 2045 across R8S5H and R4S3H, with major differences highlighted.**

Besides climate pathways, it is also critical to plan for a range of warming scenarios. Although the RCP4.5 scenarios have nearly identical fleets between the hotter and cooler warming scenarios, the RCP8.5 scenarios have notably different fleets. The hotter and cooler warming scenarios have nearly the same annual load, but the hourly loads in the hotter warming scenarios are concentrated slightly more towards the tails of the distribution. In the RCP8.5 pathway, the hotter scenarios have 16% and 21% higher renewable installations than the respective cooler scenarios. This is an early affect of climate change on load and renewable generation, and these trends will become even more severe after 2045 if the higher global emissions pathway is followed. These results also raise the issue of adaptability and mitigation. Towards the mid-century and onwards, effects of climate change are more uncertain, and so therefore are its impacts on load and generation. In turn, this can make planning more difficult, and thus require more potential investments to meet emissions targets.

2) Planning with Resiliency Periods

We present the results of two planning regimes: PRM and resiliency day planning. The PRM planning regime corresponds to the approach currently employed by the California Public Utilities Commission and California Energy Commission for their decarbonization planning studies [2]. The performance is evaluated using two scenarios. The R8S5C scenario is the closest match in terms of yearly load to California Energy

Commission's most recent integrated energy policy report (IEPR) load forecasts. The R4S3H is the next closest match, but has slightly lower loads. For reliability considerations, we merge the hotter and cooler pathways together. In other words, to convey the variability of a warming climate, both cooler and hotter perturbations are used for the determination of PRM and selection of resiliency periods. Representative periods, however, are chosen for R8S5C and R4S3H.

We compare the results of these techniques in three ways. The first is the comparison of total cost, as well as direct comparison of fleet composition. The second is the loss-of-load-expectation of each fleet. The third is a study of what margin above the peak load could be served by each fleet.

TABLE 2. Costs, billions 2025$

	R8S5C		R4S3H	
	PRM	Resil.	PRM	Resil.
Total Cost	365.7	351.2	329.6	322.8
CA Cost	214.9	200.6	179.3	173.3
Maint. Cost	34.8	33.1	29.6	27.6
Inv. Cost	162.3	150.6	131.4	127.8
CA Op. Cost	17.8	16.8	18.3	17.9

As shown in Table 2, in the R8S5C scenario, the cost savings for resilient planning over PRM is extremely substantial, over 14 billion or 6.7% in CA costs. This is mostly due to the avoided installation of several GW of thermal capacity. The R4S3H scenario presents moderately lower savings, 6 billion or 3.3%. The savings come primarily from avoided maintenance costs of economically-retired power plants and, to an extent, avoided installation of thermal capacity. This scenario has overall lower loads, so there are overall lower installations necessary to meet reliability needs. As such, the cost savings are considerably lower. In both scenarios, the operating costs are slightly lower using resilient planning as the value of renewable technologies for reliability is higher, resulting in slightly higher overall capacity of these technologies.

The cumulative investments in 2045 are shown in Fig. 5 for both scenarios. We also visualize the fleet resulting from planning with no reliability requirement ("No Rel.") to help compare the planning regimes. Both scenarios show generally similar levels of renewable and storage buildout between the PRM and resilient planning regimes. In the R8S5C scenario, there is a slight increase in renewable and slight decrease in storage build for resilient planning. In the R4S3H scenario, the renewable buildout is nearly the same, but the storage buildout is slightly higher. The key difference between the three regimes is the level of retirement and construction of thermal technology. Without any reliability, there are considerable retirements. PRM encourages heavy buildout of thermal units and nearly no retirements. Resilient planning is a middle ground between the two results. The overall lower reliance on thermal units in the two scenarios manifests in different ways. The total thermal fleets in 2045 are shown in Fig. 6, including both existing units, planned retirements, economic retirements, and new construction. Not shown are

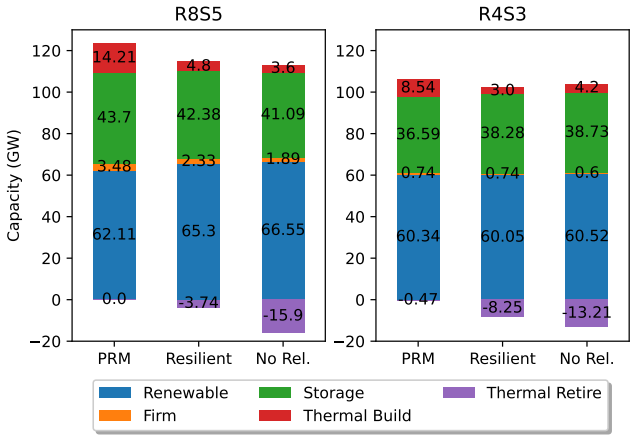

FIGURE 5. Comparison of fleets resulting from planning with PRM, the proposed resiliency days modeling, and no reliability requirement. The proposed method is less dependent on thermal units for reliability.

combustion turbine and reciprocating engine capacities which have negligible installed capacities in all scenarios. Planned retirements are minor, consisting of 2 peakers in all scenarios. Generally, combined-cycle gas turbines (CCGTs) are leveraged more heavily in 2045. In the PRM scenarios, CCGTs are the main candidate for new construction. While two smaller candidate units (steam turbine, reciprocating engine) are available, there is nearly no construction of these resources as the CCGT has a slightly lower $/MW capital cost. These resources are almost exclusively used to satisfy the reliability constraints, so their operating characteristics are less important than their capital cost in this context. These units are not visualized here due to that lack of utilization. Peakers see more retirements in general; these resources are particularly expensive to run, so pose little benefit to normal operation. However, the maintenance costs are low compared to capital costs of new construction, so peakers are retained when they serve to satisfy reliability constraints. In the lower-load R4S3H scenario, both CCGT and peakers see retirement. We have demonstrated that the fleets produced by the resilient planning regime are more economical than the PRM fleets. It is critical to demonstrate that the fleet meets the required level of reliability; otherwise, these cost savings are worthless. We seek to demonstrate that our planning approach leads to more economical, sufficiently-reliable fleets by more appropriately accounting for the load-serving potential of all resources during extreme load events. In order to demonstrate this, we directly look at the loss of load expectation. Then, the level of load above these events that could be actually served by each fleet is examined.

For each of the investment years, 10 years of unit dispatch are used, with 5 each corresponding to the cooler and hotter warming scenarios, and look for any load shedding. Neither planning regime experiences any load shedding in this test. This should come as no surprise; dispatch of extreme load periods was directly modeled in the resilient planning regime, and the PRM regime has even higher capacities. This study

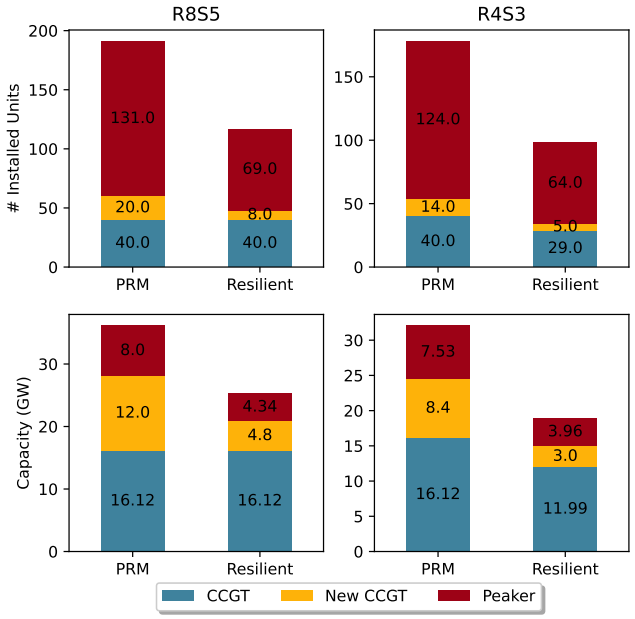

FIGURE 6. **Comparison of thermal fleet components under PRM and resiliency days modeling.**

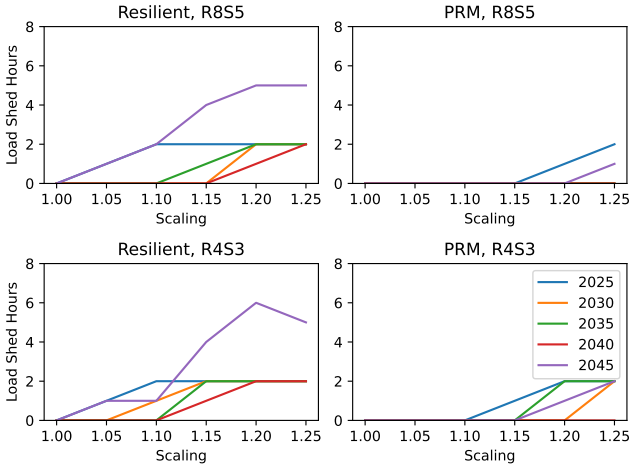

FIGURE 7. **Study showing the load shedding behavior of fleets resulting from PRM and the proposed method as the peak load day is scaled higher.**

thus satisfies the 1-in-10 loss of load expectation which informs CAISO's reliability margin.

Although this analysis is not shown, it is worth noting that if only the 1-hour gross load peak is selected for resilient planning, load shedding actually does occur in this dispatch stage. This highlights the importance of looking at the correlation between renewable generation and load rather than load alone for reliability considerations, as well as selecting net load peaks of several time scales as the resiliency periods.

It was shown that each fleet meets the reliability requirements; now we seek to demonstrate the degree to which each fleet exceeds the reliability requirements. We conduct a study showing the level of load above the peak load that could be served by each fleet. First, the 1-in-10 load day for each investment year is selected. As is, this represents a reliability threshold. Then, the load of this day is increasingly scaled and look to the number of hours with load shedding. The results of this experiment are shown in Fig. 7. The resilient planning regime typically starts requiring load shed after a 5% or 10% increase in the load. The PRM regime starts shedding load at significantly higher percentages in every case. It also experiences fewer hours of load shedding. In the R8S5C scenario, the PRM regime can meet demand 25% higher than the 1-in-10 load in 3 out of the 5 investment years. This demonstrates that the PRM scenario is overbuilt.

The key result of this analysis is that the existing method, rather than meet the prescribed reliability standard, far exceeds it. On the other hand, the proposed method more accurately tailors the portfolio to meet the reliability standard, at a lower overall cost. While higher levels of reliability are not adverse, significantly exceeding reliability standards by maintaining or building excess capacity is not the most efficient investment. In this sense, the proposed method is an improvement, as it meets reliability targets at significantly reduced costs. Finally, the proposed method is flexible, and could readily be applied to meet more or less stringent reliability targets by adjusting the specified probabilistic set of days D.

As previously discussed, the PRM constraint is artificial in the sense that it attempts to distill complex energy resource dispatch information into a single constraint. In the theoretically most rigorous planning model, thousands of days would be simulated. Periods of extreme weather, across a variety of patterns, would be directly simulated, and thus the resiliency requirements would be met. However, this type of analysis is currently infeasible due to computational limitations. The proposed method essentially occupies a subspace of that theoretical planning model. PRM-based models, however, transform into an entirely separate model by the addition of this constraint, and so the decisions made are of unknown optimality compared to real operations.

C. POLICY IMPLICATIONS

The key takeaway of this study is that PRM-based reliability requirements are too inflexible. Feasibly, PRM-based constraints could suffer from the opposite problem as well, failing to account for severe energy droughts. This problem is demonstrated by the fact that resilient planning using only the peak load day produces a fleet that has to shed load on days with lower gross load, but also less renewable generation.

In this case, the use of PRM results in chronic underestimation of renewables' contributions towards reliability. This in turn creates an artificial demand for new power plants, and a lack of retirement of existing power plants. The lack of retirement has considerable social implications. The resiliency regime retires roughly 60 peakers more than the PRM regime in both scenarios. Peakers are often located in densely-inhabitated areas [27], so reducing the reliance on these resources may have an even greater social impact

than reducing system-wide carbon emissions. Retiring these resources may have further social benefits if the land can be converted to other uses, such as housing or greenspaces. If the state moves forward under the assumption that no existing power plants will be retired, these potential benefits will be left untapped.

On the other hand, the construction of new power plants is associated with considerable embodied carbon emissions. Even if these resources never turn on, and thus never emit, in the context of normal operation, there is a notable cost associated with their construction. We follow two estimates of the emissions associated with power plant construction to obtain estimates of 450 and 1280 tons per MW [28], [29]. For the R8S5C scenario, the PRM regime is associated with an additional 3.2-9.2 million tons of emissions. Simultaneously, the 2045 emissions target is approximately 12 million tons. Although embodied emissions are not considered as part of the energy sector emissions targets, the scale of emissions associated with this capacity that is built but not required to meet reliability needs is extremely relevant. Thus, it is crucial that resources not be overbuilt, not just for cost reduction, but for a holistic view of satisfying California's climate goals.

Long-term planning models like the present model have a separate objective from short-term planning models. The goal of long-term planning models is not to determine exactly how much capacity of each resource will be purchased for the next 20 years. The goal is to determine long-term trends in capacity. Especially from the perspective of state agencies, understanding these trends is critical as they inform at a high level the implementation of various programs. The use of PRM can affect this in several ways. Thermal capacity becomes more favorable and renewable capacity is undervalued, leading to severely overbuilt fleets. The excess of thermal capacity has both cost and social ramifications. PRM also undervalues the reliability contributions of renewable and storage capacity to the extend that it reduces the amount of investment in these technologies.

It is necessary to note that reliability studies, in particular in CAISO, encompass a large number of contingencies, some of which are not suitable to be modeled here. We are not advocating for the replacement of near-term resource adequacy studies by the proposed resiliency period modeling. However, we suggest that for the task of long-term planning, the current planning reserve margin studies may be overly rigid, and undervalue the combined value of storage, wind, and solar. This is of interest to policymakers, because these long-term planning models are not directly informing utilities which resources they should buy, but informing state agencies where regulatory and funding efforts should be directed over the next decades.

We would also like to point out that the proposed resiliency days method is ultimately a data driven method. The method is effectively driven by the available projections and statistical analysis of weather-generation-load patterns. More or less frequent events could be chosen as the resiliency days, in line with the desired loss-of-load expectation. The resiliency days could also incorporate modeling for generator outages, line outages, and other climate-related risks. The key advantage of the proposed method is direct simulation of low-likelihood events. The specific implementation is flexible.

Simultaneously, the resiliency days method is enabled by the Lagrangian relaxation-based solution methodology, which provides substantial improvements in CPU time over traditional optimization solvers used alone. This technique allows us to solve a detailed dispatch model without sacrificing the temporal scope.

A caveat of these studies is that perfect foresight to which climate pathway will occur is impossible. This highlights the need for study of a range of pathways, as well as the importance of repeating these studies every few years to ensure that the trajectories take advantage of the best available science. Conversely, the advantage of the proposed resiliency days method is that it better represents the capacity needed to ensure reliability. The excess capacity held in the PRM scenarios, although unintentional, could be advantageous if the future loads are greater than the projection. However, we suggest that this type of uncertainty can be more robustly handled through scenario analysis, rather than unintended effects of PRM. Finally, we analyze a range of scenarios concerning climate and emissions, but do not consider various other uncertainties, including the future price of storage and renewable technologies, adoption of hydrogen fuels, increased energy efficiency, and so on. These factors are all relevant to a holistic understanding of future power system operations and investment in California.

V. CONCLUSION

In this paper, we investigate the impacts of climate and socioeconomic scenario uncertainty on California's decarbonization pathways. First, we formulate decarbonization planning as a MILP problem. We propose a novel method for ensuring reliability, referred to as resiliency period planning. Then, we discuss the surrogate Lagrangian relaxation-based technique that enabled computational tractability of this large MILP model. We present the results of planning under a range of climate and socioeconomic scenarios and show that the range of required new capacity of renewables and storage varies on the order of 52GW. We then compare the traditional approach to reliability to the proposed method and find that the proposed method meets the required reliability threshold at costs savings of 6.7% by more rigorously valuing the contribution of renewable technologies. This study, however, presents a limited version of the reliability studies performed by regulators and utilities. Future work will expand upon the reliability studies to further investigate the comparative performance of the proposed method and planning reserve margin-based approaches. It is also acknowledged that the direct adoption of this proposed technique has significant hurdles for the risk-adverse utility industry. Instead, we hope that this study elucidates the shortcomings of the existing methods.

REFERENCES

[1] Edison International. Countdown to 2045: Realizing california's pathway to net zero. https://www.edison.com/our-perspective/countdown-to-2045, 2023.

[2] Energy + Environmental Economics. Inputs & assumptions: 2019-2020 integrated resource planning. https://www.cpuc.ca.gov/-/media/cpuc-website/divisions/energy-division/documents/integrated-resource-plan-and-long-term-procurement-plan-irp-ltpp/2019-2020-irp-events-and-materials/inputs--assumptions-2019-2020-cpuc-irp_20191106.pdf, 2019.

[3] Blue Marble Analytics. Gridpath. https://github.com/blue-marble/gridpath, 2023.

[4] National Renewable Energy Laboratory. Regional energy deployment system model 2.0 (ReEDS 2.0). https://www.nrel.gov/analysis/reeds/index.html, 2023.

[5] Osten Anderson, Nanpeng Yu, Konstantinos Oikonomou, and Di Wu. On the selection of intermediate length representative periods for capacity expansion, 2024.

[6] Andrew Reimers, Wesley Cole, and Bethany Frew. The impact of planning reserve margins in long-term planning models of the electricity sector. *Energy Policy*, 125, 10 2018.

[7] Timo Gerres, José Pablo Chaves Ávila, Francisco Martín Martínez, Michel Rivier Abbad, Rafael Cossent Arín, and Álvaro Sánchez Miralles. Rethinking the electricity market design: Remuneration mechanisms to reach high res shares. results from a spanish case study. *Energy Policy*, 129:1320–1330, 2019.

[8] Lily Chow and Simone Brant. The 2017 resource adequacy report. Technical report, California Public Utilities Commission, 2018.

[9] Simone Brant, Eric Dupré, Michele Kito, and Judith Iklé. The 2018 resource adequacy report. Technical report, California Public Utilities Commission, 2019.

[10] Nick Schlag, Zach Ming, Arne Olson, Lakshmi Alagappan, Ben Carron, Kevin Steinberger, and Huai Jiang. Capacity and reliability planning in the era of decarbonization: Practical application of effective load carrying capability in resource adequacy. Technical report, Energy + Environmental Economics, 2020.

[11] Jethro Ssengonzi, Jeremiah X. Johnson, and Joseph F. DeCarolis. An efficient method to estimate renewable energy capacity credit at increasing regional grid penetration levels. *Renewable and Sustainable Energy Transition*, 2:100033, 2022.

[12] Wesley Cole, Daniel Greer, Jonathan Ho, and Robert Margolis. Considerations for maintaining resource adequacy of electricity systems with high penetrations of pv and storage. *Applied Energy*, 279:115795, 2020.

[13] Atri Bera, Andrew Benson, and Tu Nguyen. Reliability-based sizing of energy storage for systems with very high renewable penetration. In *2023 IEEE PESGM*, pages 1–5, 2023.

[14] Elaine Hart and Ana Mileva. Advancing resource adequacy analysis with the gridpath ra toolkit: A case study of the western us. Technical report, Gridlab, 2022.

[15] Kevin Carden, Trevor Bellon, Aaron Burdick, Charles Gulian, and Arne Olson. Incremental elcc study for mid-term reliability procurement. Technical report, California Public Utilities Commission, 2023.

[16] Salman Nazir, Hisham Othman, Khoi Vu, Shiyuan Wang, Dipayan Banik, Atri Bera, Cody Newlun, Andrew Benson, and Jim Ellison. pirp: A probabilistic tool for long-term integrated resource planning of power systems. In *2022 IEEE EESAT*, pages 1–5, 2022.

[17] Ian J. Scott, Pedro M.S. Carvalho, Audun Botterud, and Carlos A. Silva. Clustering representative days for power systems generation expansion planning: Capturing the effects of variable renewables and energy storage. *Applied Energy*, 253:113603, 2019.

[18] Leander Kotzur, Peter Markewitz, Martin Robinius, and Detlef Stolten. Impact of different time series aggregation methods on optimal energy system design. *Renewable Energy*, 117:474–487, 2018.

[19] Can Li, Antonio J. Conejo, John D. Siirola, and Ignacio E. Grossmann. On representative day selection for capacity expansion planning of power systems under extreme operating conditions. *Int. J. Electr. Power Energy Syst.*, 137:107697, 2022.

[20] Ali Yeganefar, Mohammad Reza Amin-Naseri, and Mohammad Kazem Sheikh-El-Eslami. Improvement of representative days selection in power system planning by incorporating the extreme days of the net load to take account of the variability and intermittency of renewable resources. *Applied Energy*, 272:115224, 2020.

[21] Holger Teichgraeber, Lucas Elias Küpper, and Adam R. Brandt. Designing reliable future energy systems by iteratively including extreme periods in time-series aggregation. *Applied Energy*, 304:117696, 2021.

[22] Osten Anderson, Nanpeng Yu, and Mikhail Bragin. Optimize deep decarbonization pathways in california with power system planning using surrogate level-based lagrangian relaxation, 2023.

[23] Cameron Bracken, Nathalie Voisin, Casey D. Burleyson, Allison M. Campbell, Z. Jason Hou, and Daniel Broman. Standardized benchmark of historical compound wind and solar energy droughts across the continental united states. *Renewable Energy*, 220:119550, 2024.

[24] Cameron Bracken, Travis Thurber, and Nathalie Voisin. Hourly Wind and Solar Generation Profiles at 1/8th Degree Resolution. https://doi.org/10.5281/zenodo.10214348, November 2023.

[25] Andrew Jones, Deeksha Rastogi, Pouya Vahmani, Alyssa Stansfield, Kevin Reed, Travis Thurber, Paul Ullrich, and Jennie Rice. Continental united states climate projections based on thermodynamic modification of historical weather. *Scientific Data*, 10, 09 2023.

[26] Casey Burleyson, Zarrar Khan, Misha Kulshresta, , Nathalie Voisin, and Jennie Rice. When do different scenarios of projected electricity demand start to meaningfully diverge? *Under review in Applied Energy*, 2024.

[27] Clean Energy Group. Phase out peakers: Replacing polluting urban power plants with renewables and battery storage. https://www.cleanegroup.org/publication/phase-out-peakers/, 2020.

[28] X.D. Wu, J.L. Guo, and G.Q. Chen. The striking amount of carbon emissions by the construction stage of coal-fired power generation system in china. *Energy Policy*, 117:358–369, 2018.

[29] Pamela Spath and Margaret Mann. Life cycle assessment of a natural gas combined cycle power generation system. Technical report, National Renewable Energy Laboratory, 12 2000.

OSTEN ANDERSON (Student Member, IEEE) received the B.S. degree in astrophysics from University of California at Los Angeles, Los Angeles, CA, USA in 2018, and the M.S. degree in electrical engineering from University of California at Riverside, Riverside, CA, USA in 2021. He is currently pursuing the Ph.D. degree in electrical engineering from University of California at Riverside, Riverside, CA, USA, and is a power systems research engineer at Pacific Northwest National Laboratory, Richland, WA, USA. His current research interests include power system planning and resiliency through climate change and decarbonization.

CAMERON BRACKEN received a B.S. degree in environmental resources engineering from Cal Poly Humboldt, CA, USA, in 2009, and an M.S. and Ph.D. in civil engineering from the University of Colorado at Boulder, CO, USA in 2012 and 2016, respectively. He is currently an Earth Scientist at the Pacific Northwest National Laboratory, Richland, WA, USA. His current research interests include renewable energy, hydropower, climate change and water resources forecasting.

CASEY D. BURLEYSON earned his B.S. (2007) and Ph.D. (2013) in meteorology from North Carolina State University. He is currently an Earth Scientist at Pacific Northwest National Laboratory where he has worked since 2014. Dr. Burleyson works on a broad range of topics including simulating weather and climate impacts on energy systems. He developed the open-source Total ELectricity Loads (TELL) model which simulates electricity demand in response to hour-to-hour variations in weather.

ALEX PUSCH earned his B.A. (2018) in Economics from Pomona College. He is currently an advisor for climate adaptation and resiliency planning at Southern California Edison.

NANPENG YU (Senior Member, IEEE) received the B.S. degree in electrical engineering from Tsinghua University, Beijing, China, in 2006, and the M.S. and Ph.D. degrees in electrical engineering from Iowa State University, Ames, IA, USA, in 2007 and 2010, respectively. He is currently a Professor and Vice Chair with the Department of Electrical and Computer Engineering, University of California at Riverside, Riverside, CA, USA. His research interests include machine learning in smart grid, electricity market design and optimization, and smart energy communities. He is an Associate Editor of *IEEE Transaction on Smart Grid* and *IEEE Power Engineering Letters*.